

Large Spin Alignment of the Unbound ^5He Fragment after Fragmentation of 240 MeV/nucleon ^6He

L. V. Chulkov,¹ T. Aumann,² D. Aleksandrov,¹ L. Axelsson,³ T. Baumann,⁴ M. J. G. Borge,⁵ R. Collatz,⁴ J. Cub,⁴ W. Dostal,² B. Eberlein,² Th. W. Elze,⁶ H. Emling,⁴ H. Geissel,⁴ V. Z. Goldberg,¹ M. Golovkov,¹ A. Grünschlöss,⁶ M. Hellström,⁴ J. Holeczek,⁷ R. Holzmann,⁴ B. Jonson,³ A. A. Korshennikov,⁸ J. V. Kratz,² G. Kraus,⁴ R. Kulesa,⁹ Y. Leifels,⁴ A. Leistschneider,⁶ T. Leth,¹⁰ I. Mukha,^{1,10} G. Münzenberg,⁴ F. Nickel,⁴ T. Nilsson,³ G. Nyman,³ B. Petersen,¹⁰ M. Pfützner,⁴ A. Richter,¹¹ K. Riisager,¹⁰ C. Scheidenberger,⁴ G. Schrieder,¹¹ W. Schwab,⁴ H. Simon,¹¹ M. H. Smedberg,³ M. Steiner,¹² J. Stroth,⁶ A. Surowiec,⁷ T. Suzuki,⁸ and O. Tengblad⁵

¹Kurchatov Institute, R-123182 Moscow, Russia

²Institut für Kernchemie, Johannes Gutenberg-Universität, D-55099 Mainz, Germany

³Fysiska Institutionen, Chalmers Tekniska Högskola och Göteborgs Universitet, S-412 96 Göteborg, Sweden

⁴Gesellschaft für Schwerionenforschung (GSI), D-64291 Darmstadt, Germany

⁵Instituto Estructura de la Materia, Consejo Superior de Investigaciones Científicas, E-28006 Madrid, Spain

⁶Institut für Kernphysik, Johann-Wolfgang-Goethe-Universität, D-60486 Frankfurt, Germany

⁷Institute of Physics, University of Silesia, Katowice, Poland

⁸RIKEN, 2-1 Hirosawa, Wako, Saitama 351-01, Japan

⁹Instytut Fizyki, Uniwersytet Jagielloński, PL-30-059 Kraków, Poland

¹⁰Institut for Fysik og Astronomi, Aarhus Universitet, DK-8000 Aarhus C, Denmark

¹¹Institut für Kernphysik, Technische Hochschule, D-64289 Darmstadt, Germany

¹²Michigan State University, East Lansing, Michigan 48824-1321

(Received 7 February 1997)

Peripheral fragmentation of a 240 MeV/nucleon beam of the halo nucleus ^6He incident on carbon target has been studied in a kinematically complete experiment. It is found that one-neutron stripping to the unbound nucleus ^5He is the dominant fragmentation mechanism and that it leads to a spin alignment of ^5He in a plane perpendicular to the ^5He momentum vector. This is expected to be a common feature for all neutron halo nuclei. [S0031-9007(97)03592-8]

PACS numbers: 25.60.Gc, 24.70.+s, 27.10.+h

The existence of halo states in nuclei is today a well established phenomenon, both experimentally and theoretically [1–3]. One of the main sources of information about halo states comes from investigations of fragmentation reactions. Most of these experiments have aimed at determinations of interaction cross sections, momentum distributions, and invariant mass spectra. However, elaborate studies involving spin related properties remain more or less unexplored. There is only one example [4] where experimental effects connected with the polarization of virtual photons in Coulomb dissociation of ^{11}Be have been studied.

Polarization effects in fragmentation reactions have been found experimentally a few years ago [5]. The results were described on the basis of a simple reaction mechanism in the sudden approximation: knockout of a fragment of the projectile when the remnant remains untouched. Pochodzalla *et al.* [6] failed to observe polarization of $^6\text{Li}^*(3^+)$ produced in fragmentation of ^{40}Ar due to the complicated fragmentation mechanism in this case.

The mechanism of one-neutron knockout is expected to dominate for neutron-halo nuclei since they have a spatially extended distribution of neutrons around a compact core. The polarization of the remaining fragment, which has had no active interaction with the target, is a common feature for a reaction with a noncentral interaction [7]. In

the case of a particle unstable fragment, the polarization effects manifest themselves as a characteristic angular distribution of the momenta of the decay products.

In this paper, we present new experimental data for fragmentation of a 240 MeV/nucleon beam of ^6He nuclei incident on a 1.87 g/cm² carbon target. The experiment was performed at GSI, Darmstadt, where the secondary beam was produced in a 8 g/cm² beryllium production target by a 340 MeV/nucleon primary ^{18}O beam. The produced nuclei were subsequently separated using the fragment separator (FRS) [8]. The experimental method was almost identical to the one applied in a ^8He fragmentation study described earlier [9]. Here, we just summarize the main features relevant for the analysis presented here. The direction of the incoming ion was defined by two position-sensitive multiwire proportional chambers (MWPC) placed at the entrance of the experimental cave and in front of the reaction target (angular resolution $\sigma_\theta = 0.14$ mrad). The angular distributions of charged fragments were measured by a third MWPC with a resolution $\sigma_\theta = 3.2$ mrad. Further downstream the charged fragments were deflected and analyzed in the dipole magnet ALADIN in conjunction with position-sensitive multiwire drift chambers and a plastic wall. The time of flight (TOF) between a scintillator placed at the entrance of the cave and the TOF was registered. The energy loss

in the TOF gave the charge of the detected fragment. Energy loss information was also available from two thin (500 μm) silicon pin-diode detectors placed close to the reaction target both downstream and upstream. The neutrons were detected in the large-area neutron detector (LAND) with an efficiency of $(85 \pm 2)\%$, angular resolution (σ) of about 3 mrad, and time of flight resolution 0.3%. The measured transverse momentum distributions of α particles and neutrons were effectively limited by the acceptance of the experimental setup ($-200 \text{ MeV}/c < p_{\alpha x} < 180 \text{ MeV}/c$, $-100 \text{ MeV}/c < p_{\alpha y} < 140 \text{ MeV}/c$, $-50 \text{ MeV}/c < p_{n x(y)} < 50 \text{ MeV}/c$). The selected events were coincidences between an α particle and a neutron which means that the α -particle core in ${}^6\text{He}$ has had no substantial interaction with the target and the whole process must therefore represent a peripheral collision.

The ${}^6\text{He}$ fragmentation has earlier been studied experimentally [10,11] at high energy (400 and 800 MeV/nucleon). The analysis of the transverse momentum distributions [12] has shown that the α - n final state interaction corresponding to the ${}^5\text{He}$ ground state dominates. The second neutron was found to be strongly deflected due to interaction with the target and does not make a significant contribution to the central region of the momentum distributions. The ${}^5\text{He}$ resonance is comparatively long lived ($\Gamma = 600 \pm 20 \text{ keV}$ [13], corresponding to a lifetime which is longer than 300 fm/c), and it decays therefore far away from the reaction zone. Thus a model description accounting for a sequential fragmentation to the unstable ${}^5\text{He}$ fragment followed by its decay into an α particle and a neutron is an appropriate one.

All distributions presented in this paper are given in the spectator rest frame, a coordinate system moving in the beam direction with a velocity close to the projectile velocity. This seems to be the best choice since both the experimental α -particle and neutron longitudinal momentum distributions are centered around zero in this system. Furthermore the angular distributions were found to be close to isotropic. The possibility to introduce such a system gives additional evidence that both a neutron and an α particle are coming from the same source—the decay of the unbound ${}^5\text{He}$ fragment.

Since it is known that fragment polarization is a common feature of peripheral reactions, and, in particular, nucleon-stripping reactions (see, for example, [5,14,15], and references therein), the aim was to look for such an effect in our data. In transfer reactions, the polarization phenomenon can be described by a vector of polarization perpendicular to the plane containing both the recoil nucleus (${}^5\text{He}$ in our case) and the projectile momentum vectors [7]. The decay products emitted from such a polarized nucleus show a characteristic angular distribution with respect to the polarization direction. However, other types of nonrandom orientations may occur. For example, the spin of the ejectile may be aligned in a plane, but still randomly oriented within it. The polarization vector is then equal to zero

but the momenta of the decay products are not randomly oriented. We assume here that the total angular momentum of ${}^5\text{He}$ is oriented in a direction perpendicular to the plane spanned by the projectile and the ${}^5\text{He}$ momentum vectors, $\mathbf{J} \sim \mathbf{p}^{{}^5\text{He}} \times \mathbf{p}^{\text{beam}}$. We shall then investigate if this assumption is in accordance with the experimentally observed correlations. A spin alignment of ${}^5\text{He}$ with respect to a certain direction would result in an anisotropy of the decay products relative to \mathbf{J} . It is natural to select a coordinate system with the z axis parallel to \mathbf{J} . The distribution in the case of strong polarization should be proportional to the square of a sum of the Legendre polynomials with the corresponding projections. Qualitatively, when the neutron in ${}^5\text{He}$ is in the p shell one may expect that, in a reference frame with the z axis parallel to \mathbf{J} , the dominant contributions are coming from $Y_{1,-1}^2$ and $Y_{1,1}^2$ and therefore proportional to $\sin^2 \vartheta_J$ (ϑ_J is the angle between the \mathbf{J} vector and the α - n relative momentum $\mathbf{p}_{\alpha n} = \frac{m_n m_\alpha}{m_n + m_\alpha} [\frac{\mathbf{p}_\alpha}{m_\alpha} - \frac{\mathbf{p}_n}{m_n}]$). The ${}^5\text{He}$ momentum provides another direction relative to which the decay products should have an anisotropy. One thus expects a large contribution of the $m = 0$ α - n angular momentum projection on this direction. The existence of such a special direction should result in an azimuthal anisotropy. This is illustrated in Fig. 1(a) where the open circles with error bars display the differential cross sections $d\sigma/d\cos(\vartheta_J)$ as a function of $\cos(\vartheta_J)$ and $d\sigma/d\varphi_J$ as a function of the azimuthal angle φ_J where the direction of the ${}^5\text{He}$ momentum was chosen as the x axis [Fig. 1(b)]. The shapes of the experimental distributions in Figs. 1(a) and 1(b) are in qualitative agreement with our initial assumption. Each of these distributions is, however, the result of an integration over all other kinematical variables and an unambiguous conclusion cannot be drawn.

We have therefore looked for the angular correlations in another coordinate system with the z axis parallel to the ${}^5\text{He}$ direction and the x axis in the \mathbf{J} direction. Also here a large anisotropy can be observed in the distribution of the relative momentum $\mathbf{p}_{\alpha n}$ over the polar angle $\vartheta_{\alpha n}$ [the open circles with error bars in Fig. 2(a)]. The angular dependence in this case should be given by $Y_{1,0}^2 \sim \cos^2 \vartheta_{\alpha n}$ since a large contribution of zero α - n angular momentum projection is expected. The open circles with error bars in Fig. 2(b) present the distribution obtained over azimuthal angles $\varphi_{\alpha n}$ in the same coordinate system. We observe a clear pattern in Fig. 2(a) while the shape in Fig. 2(b), as will be shown later, is an artifact of the limited acceptance of our setup, and the distribution in azimuthal angle is, in fact, isotropic. This is in contradiction with our assumption that a well defined polarization direction (\mathbf{J}) exists in a plane perpendicular to ${}^5\text{He}$ momentum direction, while it is still compatible with the assumption of an alignment.

We now proceed to an analysis in a sequential fragmentation model through the ${}^5\text{He}$ resonance using a Monte Carlo method. The ${}^5\text{He}$ momentum ($\mathbf{p}^{{}^5\text{He}} = \mathbf{p}_\alpha + \mathbf{p}_n$)

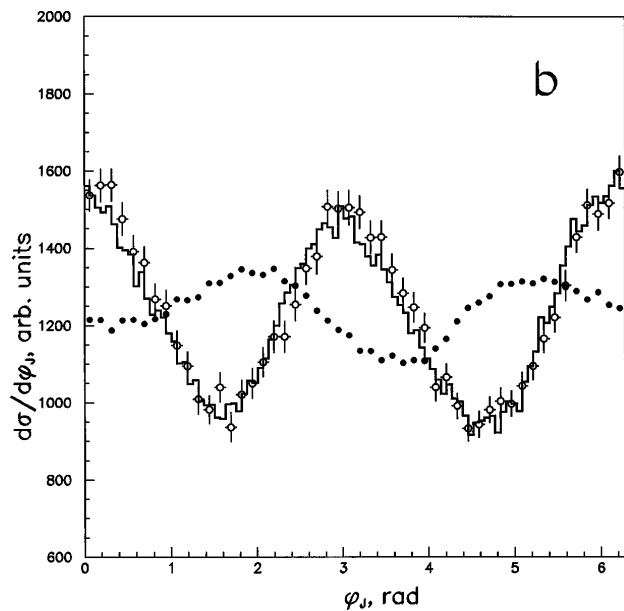
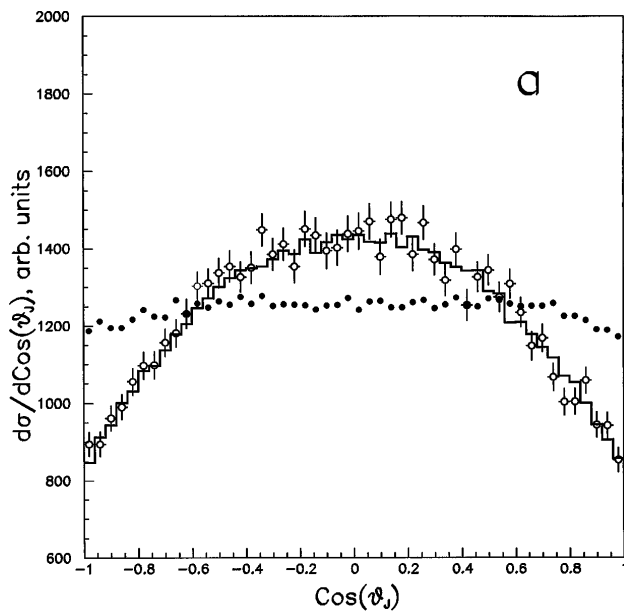


FIG. 1. Distribution of the directions of the relative momentum \mathbf{p}_{an} on the polar angle (ϑ_J) (a) and on the azimuthal angle (φ_J) (b) in the coordinate system with z axis in the direction of $\mathbf{p}^{5\text{He}} \times \mathbf{p}_{\text{beam}}$. The x axis is parallel to $\mathbf{p}^{5\text{He}}$. The experimental data are shown by the open circles with error bars. The filled circles display the result of the Monte Carlo calculations with the isotropic distribution of the decay products. The histograms present the result of the Monte Carlo calculations with the correlation function given in Eq. (1).

distribution used was obtained from the experimental data. The parameters of the $3/2^-$ resonance in the $\alpha + n$ subsystem was taken from an R -matrix analysis of n - α scattering [16]. The angular distributions of the decay products in the ${}^5\text{He}$ rest frame was, to start with, assumed to be isotropic for the spin of ${}^5\text{He}$. The experimental resolution of the α -particle and neutron momentum was taken

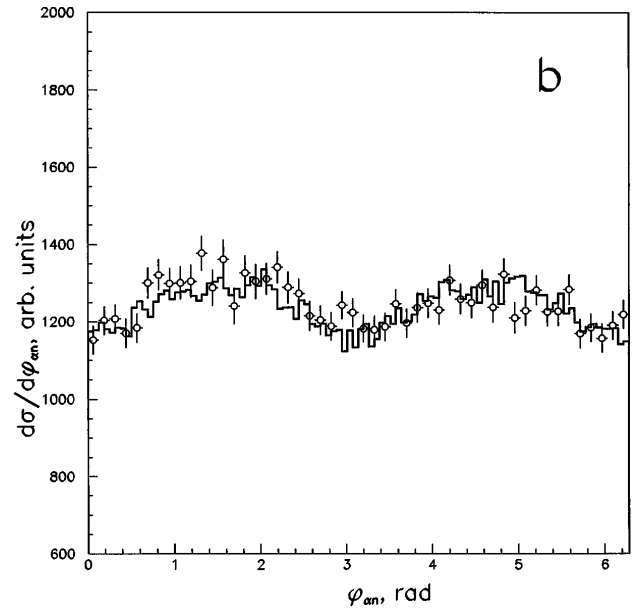
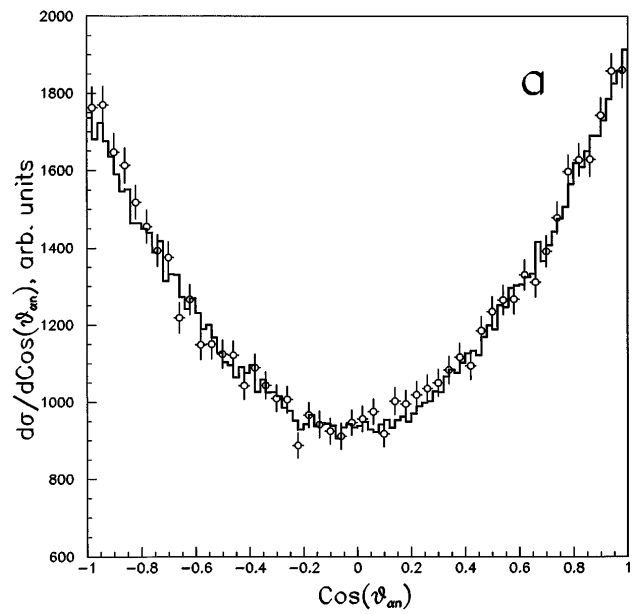


FIG. 2. Distribution of the directions of the relative momentum \mathbf{p}_{an} on the polar angle (ϑ_{an}) (a) and on the azimuthal angle (φ_{an}) (b) in the coordinate system with z axis parallel to $\mathbf{p}^{5\text{He}}$. The x axis is in the direction of $\mathbf{p}^{5\text{He}} \times \mathbf{p}_{\text{beam}}$. The experimental data are shown by the open circles with error bars. The histograms are the result of the Monte Carlo calculations with the correlation function given in Eq. (1).

into account in the simulation. The simulated kinematical variables were written event by event in a file and then analyzed in the same way as the experimental data, taking into account the acceptance of the experimental setup. The model was found to reproduce both the experimental widths and the shapes of the momentum distributions for both neutrons and α particles [17].

The differential cross sections calculated in the sequential fragmentation model is shown in Figs. 1(a) and 1(b)

by filled circles. As can be seen, the model assuming an isotropic distribution of the ${}^5\text{He}$ decay products is unable to reproduce the observed pattern. A certain structure, most pronounced in Fig. 1(b), is a result of the above-mentioned acceptance limits of the measured transverse momenta. Note that, when the restriction on the transverse momenta is removed, both distributions become isotropic. A good description of the data can, however, be obtained by introducing an anisotropy of the decay products relative to the direction of the ${}^5\text{He}$ momentum with the following shape of the correlation function:

$$W(\vartheta_{an}) \sim 1 + A \cos^2(\vartheta_{an}). \quad (1)$$

The results are shown in Figs. 1(a) and 1(b) and in Figs. 2(a) and 2(b) as histograms. The A parameter of the correlation function $W(\vartheta_{an})$ from Eq. (1) was fitted to the experimental distribution shown in Fig. 2(a). This gave $A = 1.50(3)$ (statistical error). With this value all measured differential cross sections were reproduced. The experimentally observed azimuthal anisotropy of φ_{an} , which is seen in Fig. 2(b), can be explained by the influence of the limited acceptance of the experimental setup. The correlation function used in the model does not contain any dependence on φ_{an} . This azimuthal isotropy clearly indicates that there is no special direction in a plane perpendicular to the ${}^5\text{He}$ momenta. This fact may be evidence for a spin alignment of ${}^5\text{He}$ in this plane. Such a type of alignment can be explained by the fragmentation mechanism proposed in [5].

In summary, we may conclude that one-neutron knockout is the dominating reaction mechanism in peripheral fragmentation of the halo nucleus ${}^6\text{He}$. This feature is expected to be a common feature for all nuclei having a neutron halo. For the Borromean nuclei, one-neutron knockout results in an unstable nucleus which is decaying further by neutron emission. This two-step process results in an angular correlation between the direction of the aligned recoiling unstable nucleus and its decay products. The shape of the angular correlations gives unambiguous information about the relative angular momentum between

the decay products and the structure of the unstable nucleus. This was demonstrated here with the ${}^5\text{He}$ fragment. Such structural information is, for example, very interesting for the resonances ${}^{10}\text{Li}$ and ${}^{13}\text{Be}$ where no final conclusion on their ground state structure have been made until now.

The authors acknowledge with gratitude fruitful discussions with Professor W.-D. Schmidt-Ott and Professor M. V. Zhukov. This work was supported by the BMBF under Contracts No. 06 DA 665 I, No. 06 OF 112, and No. 06 MZ 465 and by GSI via Hochschulzusammenarbeitsvereinbarungen under Contracts No. DA RICK, No. OF ELZ, and No. MZ KRK, as well as partly supported by the Polish Committee of Scientific Research under Contract No. PBZ/PB03/113/09, EC under Contract No. ERBCHGE-CT92-0003, and CICYT under Contract No. AEN92-0788-C02-02 (MJGB).

-
- [1] P. G. Hansen, A. S. Jensen, and B. Jonson, *Annu. Rev. Nucl. Part. Sci.* **45**, 591 (1995).
 - [2] I. Tanihata, *J. Phys. G* **22**, 157 (1996).
 - [3] M. V. Zhukov *et al.*, *Phys. Rep.* **231**, 151 (1993).
 - [4] T. Nakamura *et al.*, *Phys. Lett. B* **331**, 296 (1994).
 - [5] K. Asahi *et al.*, *Phys. Lett. B* **251**, 488 (1990).
 - [6] J. Pochodzalla *et al.*, *Phys. Rev. C* **35**, 1695 (1987).
 - [7] G. R. Satchler, *Introduction to Nuclear Reactions* (The Macmillan Press Ltd., New York, 1980), p. 50.
 - [8] H. Geissel *et al.*, *Nucl. Instrum. Methods Phys. Res., Sect. B* **70**, 286 (1992).
 - [9] T. Nilsson *et al.*, *Nucl. Phys.* **A598**, 418 (1996).
 - [10] T. Kobayashi, *Nucl. Phys.* **A538**, 343c (1992).
 - [11] T. Kobayashi, *Nucl. Phys.* **A553**, 465c (1993).
 - [12] A. A. Korshennikov and T. Kobayashi, *Nucl. Phys.* **A567**, 97 (1994).
 - [13] F. Ajzenberg-Selove, *Nucl. Phys.* **A490**, 1 (1988).
 - [14] R. W. Zurmuhle *et al.*, *Phys. Rev. C* **49**, 2549 (1994).
 - [15] H. Okuno *et al.*, *Phys. Lett. B* **335**, 29 (1994).
 - [16] J. E. Bond and F. W. K. Firk, *Nucl. Phys.* **A287**, 317 (1977).
 - [17] L. V. Chulkov *et al.* (to be published).